CHIN. PHYS. LETT. Vol. 38, No. 2 (2021) 020502

Micro-Gas Flow Induced Stochastic Resonance of a Nonlinear Nanomechanical Resonator

Shaochun Lin(林劭春)[1,2,3], Tian Tian(田添)[1,2,3], Peiran Yin(印沛然)[4], Pu Huang(黄璞)[4], Liang Zhang(张亮)[1,2,3*], and Jiangfeng Du(杜江峰)[1,2,3*]

[1]*Hefei National Laboratory for Physical Science at the Microscale and Department of Modern Physics, University of Science and Technology of China, Hefei 230026, China*
[2]*CAS Key Laboratory of Microscale Magnetic Resonance, University of Science and Technology of China, Hefei 230026, China*
[3]*Synergetic Innovation Center of Quantum Information and Quantum Physics, University of Science and Technology of China, Hefei 230026, China*
[4]*National Laboratory of Solid State Microstructures and Department of Physics, Nanjing University, Nanjing 210093, China*

(Received 20 October 2020; accepted 15 January 2021; published online 27 January 2021)

Fluidics is one of the most historic subjects that are well-established over centuries on the macroscopic scale. In recent years, fluid detection using a number of micro/nano scale devices has been achieved. However, the interaction of microfluid and solid devices on micro/nano-meter scale still lacks in-depth research. We demonstrate a practical nanomechanical detector for microfluidics via a string resonator with high Q-factor, suspended over a hole. This device is placed under a jet nozzle with several microns of diameter, and the interaction between the micro-gas flow and the resonator is observed by monitoring the variation of the fundamental frequency and the quality factor. Moreover, we manage to measure the fluctuations of the micro-gas flow on the nanomechanical resonator by means of stochastic resonance. This work manifests a potential platform for detecting dynamical fluid behaviors at microscopic scale for novel fluid physics.

DOI: 10.1088/0256-307X/38/2/020502

In the last few decades, nanomechanical systems have been developed as extremely sensitive sensors for detecting mass,[1–7] position,[8] force,[9–12] etc. Recently, microfluidic devices[13–15] exhibit excellent controllability in heat flux,[16] energy generation,[17,18] and display technology.[19] However, there is still a lack of effective methods to investigate micro-gas behavior. Heretofore, nanomechanical resonators have only been employed to explore oscillatory flow dynamics,[20] boundary effects,[21] chemical vapor sensors,[22] etc., where the individual micro-gas flow has not been introduced into the nanomechanical system yet. Therefore, constructing a convenient structure coupling micro-gas flow with a mechanical resonator remains challenging.

In this work, we provide a practical platform to produce micro-gas flow and measure it via a high Q-factor string resonator taken as a gas hole, so that the gas flow can pass freely without complex reflection. The gas flow is realized through a micro jet nozzle delivered by a micropipette puller. Utilizing nanopositioning systems, the position of this jet nozzle can be precisely located at top of the string resonator. Meanwhile, the frequency of resonator reduces dramatically under the influence of micro-gas flow. Moreover, we have observed the stochastic resonance in the bistable nanomechanical resonator, induced by applied modulation and the fluctuation of the flow-solid interaction. We measure the power densities of the fluctuations under varying pressure differences and obtain the linear relationship between them. This phenomenon suggests a signal amplification process from background gas noise, which inspires us to investigate micro scale fluid behaviors.[23]

Consider a nonlinear nano-mechanical resonator, fluctuated by a micro-gas flow:

$$m\ddot{x} + m\gamma\dot{x} + kx + \alpha x^3 = F_{\rm res}(t) + \xi_{\rm gas}(t), \quad (1)$$

where γ is the dissipation rate, $k = m\omega_0^2$ is the linear elastic constant, and αx^3 represents the Duffing nonlinearity with α being the cubic elastic constant (Duffing constant); $\xi_{\rm gas}$ refers to the fluctuations of micro-gas flow introduced by the jet nozzle, regarded as white noise with intensity D,[24,25] $\langle\xi(t)\xi(t')\rangle = 2D\delta(t-t')$. $F_{\rm res}(t)$ denotes the applied modulated drive force on the resonator at frequency

Supported by the National Key R&D Program of China (Grant No. 2018YFA0306600), the Chinese Academy of Sciences (Grant Nos. GJJSTD20170001 and QYZDY-SSW-SLH004), and Anhui Initiative in Quantum Information Technologies (Grant No. AHY050000).
*Corresponding authors. Email: liangzhang@ustc.edu.cn; djf@ustc.edu.cn
© 2021 Chinese Physical Society and IOP Publishing Ltd

$\omega \approx \omega_0$:

$$F_{\rm res}(t) = [F_{\rm d} + F_{\rm mod}(t)]\cos(\omega t), \tag{2}$$

where $F_{\rm d}$ refers to the drive amplitude, and $F_{\rm mod} = \delta F \cos(\Omega t)$ is a small slow modulation on $F_{\rm d}$, under the conditions of $\delta F \ll F_{\rm d}$ and $\Omega \ll \omega$.

For weak drive, the resonator behaves simply like a harmonic oscillator. However, with the drive amplitude increases, nontrivial dynamics emerges. Especially, as $F_{\rm d}$ exceeds the critical value $F_{\rm c} = (\frac{4}{3})^{5/4}\frac{\omega_0^3}{\varepsilon}\sqrt{\frac{m^3}{\alpha Q^3}}$, bifurcation occurs,[26] and the oscillation of the resonator dives into the bistable region. With a high quality factor resonator ($\gamma \ll \omega$), this bistable system can be described as an overdamped double-well model. Meanwhile, noise induced by microfluid can activate random transitions between the bi-states, with transition rate:

$$\Gamma_{\rm K} = \frac{1}{\sqrt{2}\pi} e^{-\frac{\Delta V}{D}}, \tag{3}$$

where ΔV denotes the height of the effective potential barrier. The system can approach an appropriate working point near the bifurcation point, with corresponding drive amplitude $F_{\rm d}$ and frequency ω. At the working point, the transition rate between the states are nearly equal, $\Gamma_+ \approx \Gamma_- = \Gamma_{\rm K}$. When we add a small slow modulation on the drive amplitude, this transition turns to be coherent following the modulation frequency Ω in the time domain, which indicates a peak in frequency domain after Fourier transform. The signal-to-noise ratio (SNR) in the power spectrum is defined[23] as

$$\mathrm{SNR} = \frac{2}{N(\Omega)}\Big[\lim_{\Delta\omega\to 0}\int_{\Omega-\Delta\omega}^{\Omega+\Delta\omega} S(\omega)\,d\omega\Big] = \frac{S(\Omega)}{N(\Omega)}, \tag{4}$$

where $S(\Omega)$ is the height of the power spectrum peak at the modulation frequency Ω, and $N(\Omega)$ is the spectral background. Under certain condition, the SNR reaches the max, known as the stochastic resonance phenomenon.[27] Here, SNR reads

$$\mathrm{SNR} = \pi\Big(\frac{A_0 x_m}{D}\Big)^2 \Gamma_{\rm K}, \tag{5}$$

with x_m referring to the bi-stable states, and A_0 the modulation amplitude. D is the background noise density induced by micro-gas flow. We can obtain the micro flow force density as

$$S_{\rm F} = \delta F m\omega x_m \sqrt{\frac{\pi\Gamma_{\rm K}}{\delta\omega\,\mathrm{SNR}}}. \tag{6}$$

Therefore, combining the microfluid fluctuation with nanomechanical resonator, the stochastic resonance provides a practical method for signal amplification and microfluid detection.[20–23]

Here, we build a system consisting of a string resonator with a gas hole and a tubule with micro scale jet nozzle on its outlet, as shown in Fig. 1(a). The gas nozzle is pulled about 5 μm to 10 μm diameter via a commercial micropipette puller, and stick to an 80-cm-long and 0.8-mm-diameter tubule. This tubule connects two vacuum chambers. The resonator and the outlet jet-nozzle are maintained in high vacuum environment (chamber 2 with corresponding pressure P_2, usually around 10^{-6} mbar), while the inlet of tubule is placed in high pressure environment (chamber 1 with corresponding pressure P_1), whose pressure is tunable (usually changes from 100 to 1000 mbar). Purified nitrogen is used for generating jet flow through the tubule from high pressure to the high vacuum. Meanwhile, the jet nozzle is made of fused silica glass and vertically fixed above the mechanical resonator. Piezo-based nanopositioners are employed to locate jet-nozzle in three dimensions. The scanning electron microscope photograph of the end of the nozzle is shown in Fig. 1(b), with an inner diameter of about 10 μm.

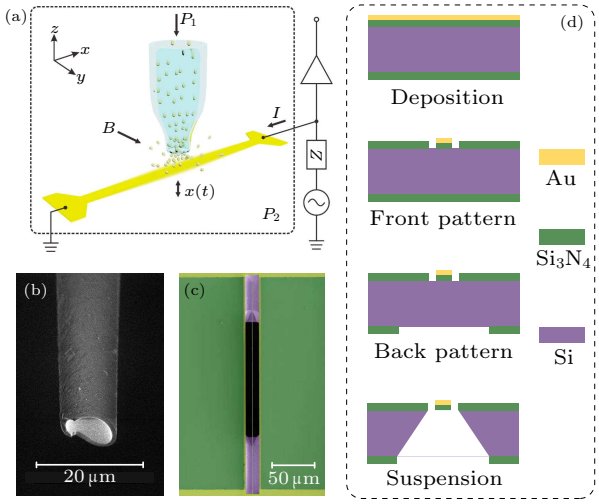

Fig. 1. Overview of the micro gas detecting system. (a) Schematic of the nanomechanical detector for micro-gas flow. This gas nozzle is approximately 5 μm to 10 μm diameter and is equipped with a nanopositioned system. The gas flow is manipulated via the pressure difference $\Delta P = P_1 - P_2$. Here, we employ two vacuum chambers with P_1 usually at around 10^3 mbar and P_2 about 10^{-6} mbar. (b) The scanning electron microscope (SEM) photograph of the end of the micro jet nozzle, showing an inner diameter of about 10 μm. (c) The SEM photograph (false color) of high Q-factor string resonator with a gas hole. The string resonator is in sizes 200 μm long, 500 nm wide and 100 nm thick, with 15 nm Au coated. (d) Nano-fabrication processes of silicon nitride string resonator with a gas hole. The gas hole is designed to let the micro-gas flow pass freely without reflection.

The size of the string resonator is 200 μm × 500 nm × 100 nm, as shown in Fig. 1(c). The eigenfrequency is about 644.6 kHz. We choose high stressed silicon nitride (>1.1 GPa) to improve the Q-factor of

the string resonator,[28–30] which can reach 10^5 at room temperature without the influence of the jet flow (10^{-6} mbar). The motion of this resonator is excited and measured via standard magneto-motive technique.[31] The resonator vibrates along the Z direction and the magnetic field is applied on the Y axis, as shown in Fig. 1(a). To be noticed, during the experiment, the distance between the jet nozzle and the mechanical resonator is so small (about 2 μm) that the gas may hit the substrate and cause a complex reflection phenomenon even before it expands into the vacuum. Therefore, to eliminate the disturbance of reflected gas from the substrate, we manage to excavate a gas hole in the middle of the resonator to make a free pass. The main fabrication processes are presented in Fig. 1(d). We choose a 100-nm-thick high-stressed (>1.1 GPa) silicon nitride film grown by low-pressure chemical vapor deposition (LPCVD) to reduce the internal consumption of string resonator. A 15 nm Au layer is sputter coated on the silicon nitride for magneto motivation.[31] Then, the e-beam lithograph is applied to pattern the string resonator, and followed up by ion beam etch (IBE) to remove the redundant metal. Afterwards, we make an ultra-violet (UV) lithography and reactive ion etch (RIE) to remove the silicon nitride at front. Later, we must overlay the pattern from backwards. Finally, the KOH is adopted to etch the entire gas hole.

In order to locate the relative position of the jet nozzle and the resonator, we monitor the frequency shift as a function of relative position, under the condition of $P_1 = 900$ mbar, $P_2 = 3.4 \times 10^{-6}$ mbar. The resonator is driven via the standard magneto-motive technique with about 1 T magnitude field, and the frequency responses are measured by a lock-in amplifier. Here, all the frequencies are normalized. As we can see in Fig. 2, there is an obvious decrease in resonance frequency and quality factor here at room temperature, which is mainly caused by gas damping.[32,33] Figure 2(a) presents the responses of resonance frequencies influenced by micro-gas flow. Peak 1 is measured when gas nozzle is far away from the resonator, in which the resonance frequency coincides with the eigenfrequency at around 644.6 kHz. Meanwhile, peak 2 is measured when gas nozzle approaches to the resonator, in which clearly decreases in resonance frequency and Q-factor are observed. Figure 2(b) illustrate the frequency response under the influence of the gas flow, while the gas nozzle is moving along the resonator by the nanopositioning system. It is clear that, when the nozzle is not close to the resonator, there is no distinct response of the frequency. However, when the nozzle is at the top of the resonator, the frequency reduces apparently. The travel length (about 200 μm) of the nanopositioning system is coincident with the length of the resonator. Analogously, on the Y direction, in Fig. 2(c), there is a decrease of frequency which fits the Lorentz shape well. The rigorous explanation of this Lorentz signal is still unclear which may be caused by the velocity distribution outside the gas nozzle. The full width half maximum is about 10 μm, which is associated with the diameter of the gas nozzle, and exhibits great collimation at the same time. The device is placed under high vacuum, where the gas flow will not propagate for a long distance, therefore, the response of the mechanical resonator is mainly resulted from the gas nozzle.

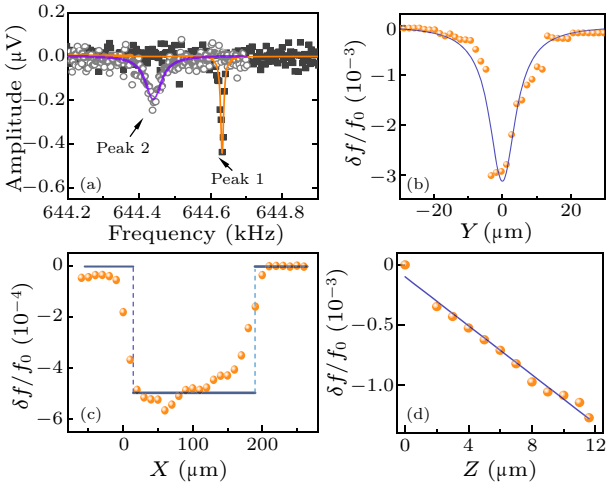

Fig. 2. Detecting the relative position of the micro jet nozzle and the string resonator via frequency responses of micro-gas flow. (a) The frequency response of mechanical resonator far away from the nozzle (black square), fitted as peak 1 (orange solid curve). When the nozzle is placed near the resonator, a shifted and widen response spectrum is measured (circle), fitted as peak 2 (purple solid curve). (b)–(d) Three-dimensional localization of micro jet nozzle, based on the relative frequency shift ratio ($\delta f/f_0$), where the data is shown as yellow dots and the guide lines are shown as purple curves. (b) Moving the nozzle along the X direction, the frequency shift occurs within a length of approximately 200 μm, corresponding to the length of string resonator. (c) Moving the nozzle along the Y direction, the frequency within around 10 μm, corresponding to the diameter of micro jet nozzle. (d) The frequency shift when the mechanical resonator approaches the nozzle along the Z direction. The zero point here refers to the original position before the approaching processes.

Figure 2(d) describes the approaching processes of the nozzle to the resonator. The zero point here refers to the original position before approaching. There is a linear relationship between the frequency shift and the distance between the nozzle and the resonator. In the experiment, we placed the nozzle near the center of the resonator by a telephoto microscope with the initial position (X, Y, Z) (μm). We first move along the Y direction, as shown in Fig. 2(c), and locate the position at $(X, 0, Z)$ (μm). Next, we move along the X direction, as shown in Fig. 2(b), and locate the position at $(100, 0, Z)$ (μm). Finally, we approach the resonator and the nozzle along the Z direction, and locate the position at $(100, 0, 11.5)$ (μm).

After the location procedure, we change the pressure of vacuum chamber 1 to strengthen the gas flow so as to produce the bi-state of the mechanical resonator. As explained in Eq. (3), bi-stable states occur when the force applied on the resonator exceeds the critical force F_c for standard Duffing oscillator, where hysteresis appears as a result of nonlinearity, as shown in Fig. 3(a) together with the inset. When we tune the frequency in the middle of the hysteresis loop and measure the amplitude dependency of time, the amplitude stays on either of the bi-stable states without transition.[27] However, taking microfluid noise into consideration, we find out that transition between those two states occurs randomly, with hopping rate $\Gamma_K = \frac{1}{\sqrt{2}\pi} e^{-\frac{\Delta V}{D}}$. As presented in Fig. 3(b), we carefully adjust the frequency to make sure that the distribution between those two stable states are equal over a long time, from which we can measure the hopping rate accurately.

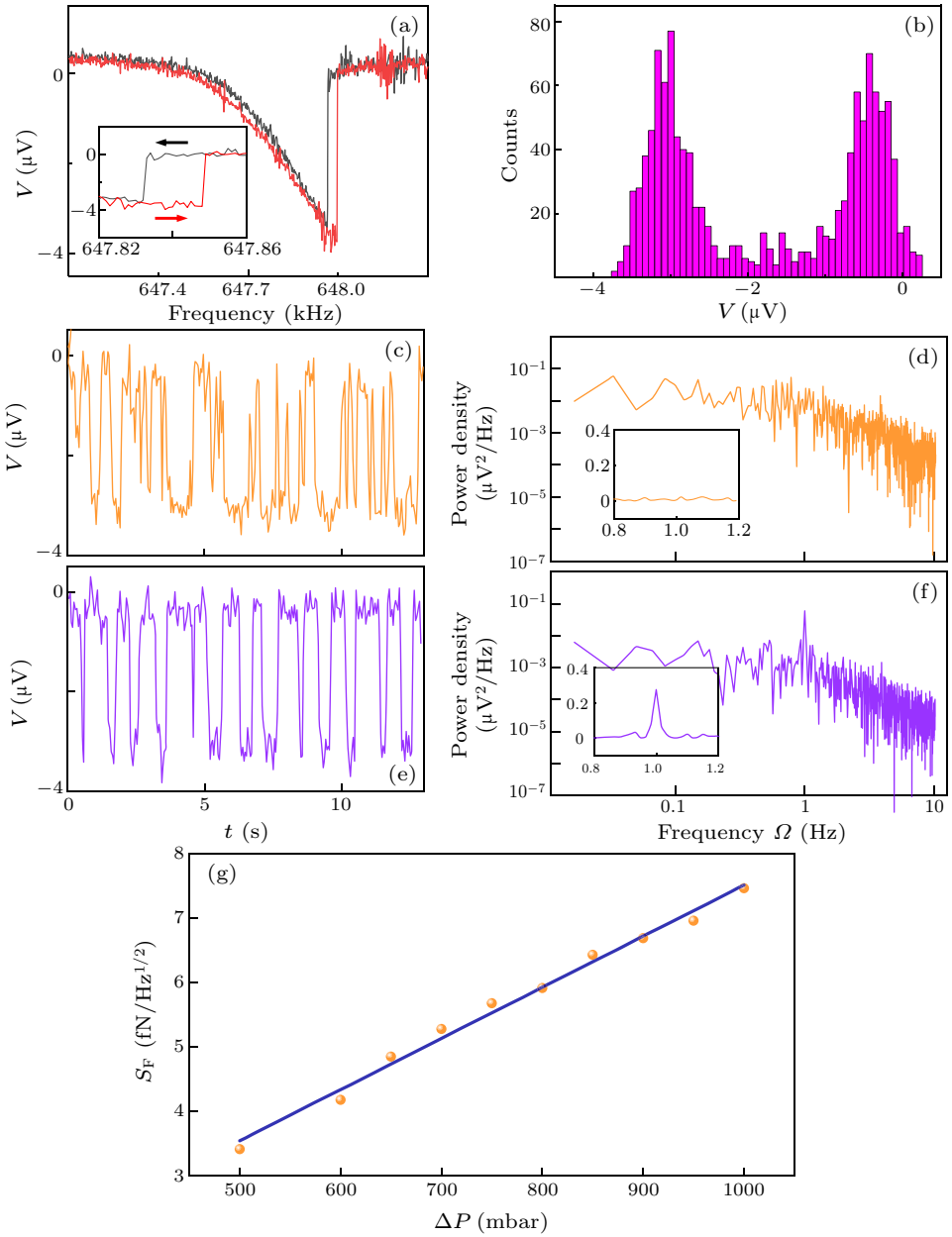

Fig. 3. Observation of stochastic resonance driven by micro-gas flow, in which incoherent gas fluctuations convert into coherent amplitude switches. (a) A typical bi-state under large drive force. The hysteresis is shown in the inset. (b) The distribution between those two stable states, counting in 60 s. (c) Observation of random transition processes induced by micro gas fluctuation for about 12.5 s. (d) The Fourier spectrum diagram of random transition regime, with no significant peak for power density. (e) Observation of stochastic resonance, modulated by $\delta F \cos(\Omega t)$, for the same 12.5 s. (f) The Fourier spectrum diagram of stochastic resonance regime, with a peak of power density at $\Omega = 1$ Hz. (g) The linear relationship between micro gas force density and the pressure. The gas force density can reach about 7.5 fN/Hz$^{1/2}$, which is much stronger than thermal noise, estimated below 1 fN/Hz$^{1/2}$. The zoomed-in insets in (d) and (f) clearly illustrate the peak of power density at 1 Hz.

In the time domain, we observe this random transition induced by micro gas fluctuations for about 12.5 s in Fig. 3(c). Under such circumstance, the so-called stochastic resonance is employed to enhance the signal from random transition to periodic resonance, as presented in Fig. 3(e), another observation of periodic resonance for about 12.5 s, with modulation amplitude δF and frequency Ω. As we can see in Fig. 3(d), when $\Omega = 0$, which refers to the random transition regime, the Fourier spectrum diagram shows no peak. However, in Fig. 3(f), the power spectrum reveals that at $\Omega = 1$ Hz, the power density reaches the peak, with the maximum energy power density around 0.5 $\mathrm{mV}^2/\mathrm{Hz}$. In this way, the incoherent background fluctuation converts into coherent switches of those bi-stable states. Moreover, we measure the force density of the micro-gas flow under different pressures, followed by Eq. (6), and obtain the linear relationship between them, as shown in Fig. 3(e). The maximum force is about 7.5 $\mathrm{fN}/\mathrm{Hz}^{1/2}$ at 1000 mbar, which indicates the signal amplification by micro-gas flow.

In conclusion, we have presented a micro-gas flow into a nanomechanical resonator system. The string resonator with a gas hole is designed to explore gas properties without reflecting disturbances, which blaze a path towards micro scale fluid-structure interaction. Meanwhile, by monitoring the frequency shift of the string resonator, the relative position of micro-gas flow and string resonator can be located precisely within several microns via a nanopositioning system. Moreover, we observe the stochastic resonance induced by the micro-gas flow. The incoherent gas fluctuation converts into coherent switches through a weak periodic modulation. Finally, the linear relationship between gas force density and pressure is measured utilizing this nanomechanical detector. This nanomechanical-microfluid coupling system provides a practical platform for investigating fundamental hydromechanics at microscale.

This work was partially carried out at the USTC Center for Micro and Nanoscale Research and Fabrication.

References

[1] Zhang Y and Zhao Y P 2015 *Sensors* **15** 14871
[2] Jensen K, Kim K and Zettl A 2008 *Nat. Nanotechnol.* **3** 533
[3] Lassagne B, Garcia-Sanchez D, Aguasca A and Bachtold A 2008 *Nano Lett.* **8** 3735
[4] Chaste J, Eichler A, Moser J, Ceballos G, Rurali R and Bachtold A 2012 *Nat. Nanotechnol.* **7** 301
[5] Yang Y T, Callegari C, Feng X L, Ekinci K L and Roukes M L 2006 *Nano Lett.* **6** 583
[6] Naik A K, Hanay M S, Hiebert W K, Feng X L and Roukes M L 2009 *Nat. Nanotechnol.* **4** 445
[7] Chiu H Y, Hung P, Postma H W C and Bockrath M 2008 *Nano Lett.* **8** 4342
[8] LaHaye M D 2004 *Science* **304** 74
[9] Rugar D, Budakian R, Mamin H J and Chui B W 2004 *Nature* **430** 329
[10] Huang P, Zhou J, Zhang L, Hou D, Lin S, Deng W, Meng C, Duan C, Ju C, Zheng X, Xue F and Du J 2016 *Nat. Commun.* **7** 11517
[11] Bordag M, Mohideen U and Mostepanenko V 2001 *Phys. Rep.* **353** 1
[12] Smullin S J, Geraci A A, Weld D M, Chiaverini J, Holmes S and Kapitulnik A 2005 *Phys. Rev. D* **72** 122001
[13] Squires T M and Quake S R 2005 *Rev. Mod. Phys.* **77** 977
[14] Whitesides G M 2006 *Nature* **442** 368
[15] Hong J W and Quake S R 2003 *Nat. Biotechnol.* **21** 1179
[16] Zhang L, Koo J M, Jiang L, Asheghi M, Goodson K E, Santiago J G and Kenny T W 2002 *J. Microeletromech. Sys.* **11** 12
[17] Esquivel J P, Campo F J D, de la F J L G, Rojas S and Sabaté N 2014 *Energy & Environ. Sci.* **7** 1744
[18] Ferrigno R, Stroock A D, Clark T D, Mayer M and Whitesides G M 2002 *J. Am. Chem. Soc.* **124** 12930
[19] Roques-Carmes T, Hayes R A, Feenstra B J and Schlangen L J M 2004 *J. Appl. Phys.* **95** 4389
[20] Bullard E C, Li J, Lilley C R, Mulvaney P, Roukes M L and Sader J E 2014 *Phys. Rev. Lett.* **112** 015501
[21] Defoort M, Lulla K, Crozes T, Maillet O, Bourgeois O and Collin E 2014 *Phys. Rev. Lett.* **113** 136101
[22] Bargatin I, Myers E B, Aldridge J S, Marcoux C, Brianceau P, Duraffourg L, Colinet E, Hentz S, Andreucci P and Roukes M L 2012 *Nano Lett.* **12** 1269
[23] Badzey R L and Mohanty P 2005 *Nature* **437** 995
[24] Aldridge J S and Cleland A N 2005 *Phys. Rev. Lett.* **94** 156403
[25] Lotze C, Corso M, Franke K J, von Oppen F and Pascual J I 2012 *Science* **338** 779
[26] Lifshitz R and Cross M C 2008 *Reviews of Nonlinear Dynamics and Complexity* (New York: Wiley-VCH Verlag) chap 1
[27] Gammaitoni L, Hänggi P, Jung P and Marchesoni F 1998 *Rev. Mod. Phys.* **70** 223
[28] Schmid S, Jensen K D, Nielsen K H and Boisen A 2011 *Phys. Rev. B* **84** 165307
[29] Verbridge S S, Parpia J M, Reichenbach R B, Bellan L M and Craighead H G 2006 *J. Appl. Phys.* **99** 124304
[30] Unterreithmeier Q P, Faust T and Kotthaus J P 2010 *Phys. Rev. Lett.* **105** 027205
[31] Cleland A and Roukes M 1999 *Sens. Actuators A* **72** 256
[32] Verbridge S S, Craighead H G and Parpia J M 2008 *Appl. Phys. Lett.* **92** 013112
[33] Verbridge S S, Ilic R, Craighead H G and Parpia J M 2008 *Appl. Phys. Lett.* **93** 013101